Article

J. Biol. Regul. Homeost. Agents. 2024; 38(5): 4361–4373
https://doi.org/10.23812/j.biol.regul.homeost.agents.20243805.346

mTORC1-ATF4-MCP-1 Pathway as a Driver of Chronic Thromboembolic Pulmonary Hypertension in Rats through the Induction of Endothelial Dysfunction and Pulmonary Artery Thromboembolism

Jinyan Shao[1,†], Yang Li[1,†], Yanyan Li[1], Fupeng Wu[1], Zichen Xie[1,*], Keyu Sun[1,*]

[1]Emergency Department, Minhang Hospital, Fudan University, 201199 Shanghai, China
*Correspondence: x_zc@fudan.edu.cn (Zichen Xie); sunkeyu@fudan.edu.cn (Keyu Sun)
[†]These authors contributed equally.
Published: 1 May 2024

Background: Chronic thromboembolic pulmonary hypertension (CTEPH) is a debilitating condition caused by a putative mechanism associated with the activation of the mammalian target of rapamycin (mTOR). The current study aims to unravel the signaling pathway leading to CTEPH on the basis of mTOR activation.
Methods: *In vivo* CTEPH models were established from rats exposed to repeated autologous thromboembolization. The rats were subjected to right ventricular pressure (RVP) and mean pulmonary artery pressure (mPAP) measurement as well as histopathological examination. To establish CTEPH cellular models for *in vitro* experiments, pulmonary artery endothelial cells were isolated from CTEPH rats and identified via immunofluorescence/flow cytometry. AZD8055, an mammalian target of rapamycin complex 1 (mTORC1) inhibitor, was used to treat both *in vivo* and *in vitro* models. Activating transcription factor 4 (ATF4) was overexpressed in *in vitro* models. Viability and apoptosis were detected using cell counting kit-8 assay and flow cytometry. Expression of mTOR, ATF4 and monocyte chemoattractant protein-1 (MCP-1) in pulmonary artery tissues/cells was measured by means of immunohistochemistry, Western blotting, quantitative reverse transcription polymerase chain reaction (qRT-PCR), and enzyme-linked immunosorbent assay (ELISA). The interaction between ATF4 and MCP-1 was predicted with bioinformatics approach and validated using Chromatin immunoprecipitation (ChIP) assay.
Results: CTEPH rats exhibited elevated mPAP, activated mTORC1-ATF4-MCP-1 pathway, increased area/total area of pulmonary artery, and enhanced apoptosis and thromboembolism in the pulmonary artery tissues, which were all reversed by AZD8055 treatment. In *in vitro* models, ATF4 overexpression decreased cell viability, enhanced apoptosis and upregulated MCP-1 level, while AZD8055 exerted an opposite effect, normalizing these changes and suppressing the mTORC1-ATF4-MCP-1 pathway. ATF4 could bind to MCP-1 promoter region.
Conclusion: The mTORC1-ATF4-MCP-1 pathway induces endothelial dysfunction and pulmonary artery thromboembolism to promote the development of CTEPH in rats.

Keywords: chronic thromboembolic pulmonary hypertension; mTORC1; ATF4; MCP-1; endothelial dysfunction

Introduction

Chronic thromboembolic pulmonary hypertension (CTEPH) is a debilitating condition, arising from thrombotic material-induced pulmonary arterial obstruction following pulmonary embolism (PE) [1]. Pathologically, CTEPH is caused by thromboembolic material that further results in altered vascular remodeling. These pathologies are collectively triggered or enhanced by impaired fibrinolysis, defective angiogenesis, and endothelial dysfunction, and can ultimately lead to right ventricular failure and death [2]. Currently, the precise pathomechanisms underlying CTEPH have yet to be fully elucidated.

Endothelium, the lining of vessel wall constituted by endothelial cells, is involved in the development of CTEPH, when dysfunctional, and plays a causative role in promoting pulmonary thromboembolism and vascular remodeling [3]. In CTEPH, endothelial cell dysfunction and pulmonary arterial tissue remodeling are associated with genetic and molecular alterations [4]. The mammalian target of rapamycin (mTOR), a serine/threonine kinase from phosphoinositide 3-kinase (PI3K) family, modulates protein and lipid biosynthesis, cell cycle transition, survival, proliferation, apoptosis and senescence [5,6]. These molecular and cellular functions, however, become aberrantly controlled during endothelial dysfunction and vascular remodeling [7]. mTOR, as an important signaling protein, participates in these phenotype changes via the PI3K/AKT kinase pathway [8]. mTOR is well-known for its pro-proliferative role with its ability to link activated signaling pathways

Journal of
BIOLOGICAL REGULATORS
and Homeostatic Agents

necessary for cell growth and proliferation [9,10]. By interacting with different proteins, mTOR can form two distinct complexes, mammalian target of rapamycin complex 1 (mTORC1) and mTORC2, of which mTORC1 primarily contributes to cell growth, inhibits autophagy and promotes the synthesis of nucleotides under stressful conditions [11]. Notably, based on existing research, the inhibition of mTOR attenuates pulmonary vascular remodeling in patients with CTEPH [12]. Suppressed mTORC1 activity is linked to the attenuated vascular remodeling in pulmonary arterial hypertension [13]. Activated mTORC1 may trigger endothelial dysfunction via reactive oxygen species signaling [14]. However, whether mTORC1 activation induces endothelial dysfunction and vascular remodeling to boost CTEPH progression remains enigmatic.

Activating transcription factor 4 (ATF4), a basic leucine zipper (bZIP) transcription factor, is involved in the selective transcription of genes based on cellular stress, and thus trigger the transcription of genes implicated in adaptation to stress [15]. The expression of ATF4 is increased in response to the enhanced endoplasmic reticulum (ER) stress and inhibited protein folding, both of which drive homocysteine-induced endothelial dysfunction [16]. A previous study has reported that mTORC1 activates ATF4 to trigger purine synthesis [17]. Recently, mTORC1 has been documented to promote protein and glutathione synthesis downstream of growth signals by activating ATF4 [18]. These reported findings suggest that mTORC1 may activate ATF4 to trigger endothelial dysfunction in CTEPH.

Monocyte chemoattractant protein-1 (MCP-1) from the C-C chemokine family is a key chemokine regulating the migration and infiltration of monocytes or macrophages [19]. Upregulation of MCP-1 has previously been observed in endothelium within neointima of the hypertensive large elastic pulmonary artery and correlated with increased pulmonary vascular resistance in CTEPH [20]. At present, ATF4 is identified as a positive regulator of MCP-1 in microvascular endothelial cells and able to promote inflammatory cell infiltration to induce endothelial injury [21].

Taken together, these prior findings contribute to a hypothesis that mTORC1 activation may activate ATF4 to initiate MCP-1 transcription, thereby causing endothelial dysfunction and further vascular remodeling in CTEPH. To test this hypothesis, we constructed animal and cellular models using rats and endothelial cells, respectively, in this study.

Methods and Materials

Establishment of Murine Model of CTEPH

Clean-grade male Sprague-Dawley rats (n = 60; 2-month-old) were procured from Hangzhou Medical College (Hangzhou, China), and bred in an animal house under a specific pathogen-free environment adjusted at a room temperature of 24 ± 0.5 °C and 60 ± 5% relative humidity, and on a 12/12-hour circadian schedule. The animals were given access to food and water *ad libitum*.

The rats were randomly divided into four groups (n = 15 per group) according to presence of CTEPH condition and type of treatment: Sham, CTEPH, CTEPH + dimethyl sulfoxide (DMSO), and CTEPH + AZD8055 groups. CTEPH was induced by exposing rats to repeated autologous thromboembolization, a process conducted according to a previously published method [22]. Briefly, the rats were anesthetized by inhalation of isoflurane (PHR2874, 3%; Sigma-Aldrich, St. Louis, MO, USA), followed by blood collection from their retro-orbital veins. After 24 h, the blood samples were washed with normal saline and then made into thrombus columns (1 mm × 3 mm). The thrombus columns (32 ± 5 sticks) were reacted with tranexamic acid (100 mg/mL; 1672745, Sigma-Aldrich, St. Louis, MO, USA) in 2 mL normal saline before being injected into animals using a syringe. Under anesthesia, the rats from the CTEPH, CTEPH + DMSO, and CTEPH + AZD8055 groups were injected with the thrombus columns in the left external jugular vein and intraperitoneally with tranexamic acid (200 mg/kg/day). To avoid infection, these animals were also given intramuscular injection of penicillin (100,000 U/kg/day). The rats in the Sham group received injection with normal saline of the amount identical to that of the injected autologous thrombus and tranexamic acid. The procedures were repeated on the 4th and 11th day after the first embolization. The increased right ventricular pressure (RVP) and mean pulmonary artery pressure (mPAP) provide indications regarding the success of model construction; the representative result is shown in Fig. 1.

To investigate how mTORC1 activation is associated with the pathology of CTEPH, rats from the CTEPH + AZD8055 group were treated with AZD8055 (HY-10422, MedChemExpress, Monmouth Junction, NJ, USA) previously dissolved in dimethyl sulfoxide (DMSO; D8418, Sigma-Aldrich, St. Louis, MO, USA), which was administered via intraperitoneal injection (5 mg/kg/day) [23]. In CTEPH + DMSO group, the rats were injected with the same amount of DMSO instead after CTEPH induction. At the 1st, 2nd and 4th week after the first pulmonary embolization, three rats were taken from the Sham and CTEPH groups, respectively, and euthanized via spinal dislocation under anesthesia realized through intraperitoneal injection of pentobarbital sodium (P010, 1%, 45 mg/kg; Sigma-Aldrich, St. Louis, MO, USA), and rat left pulmonary tissues were harvested and used for molecular analysis.

Measurement of Right Ventricular Pressure and Mean Pulmonary Artery Pressure

After the rats were anesthetized via inhalation of 3% isoflurane, the right ventricular pressure (RVP; green arrow in Fig. 1) and mean pulmonary artery pressure (mPAP; blue arrow in Fig. 1) of rats were measured by a murine non-invasive blood pressure monitor (BP-98A, Softron Biotechnology, Beijing, China) and pinpointed from the waveform

curve. In brief, a self-made rat-specific right heart catheter was slowly pushed into the right ventricle and pulmonary artery through the right external jugular vein. The catheter was connected to the murine non-invasive blood pressure monitor through a pressure transducer to directly observe and record the RVP and PAP of the rat. Afterward, the rats from all the groups were sacrificed under anesthesia, and the left pulmonary tissues were collected for histopathological examination, apoptosis detection and molecular analysis.

Histopathological Examination

The isolated left pulmonary tissues were examined for pulmonary thromboembolism with naked eyes. Then, the tissues were subjected to 24 h of fixation (4% paraformaldehyde, 16005, Sigma-Aldrich, St. Louis, MO, USA), dehydration (gradient ethanol), hyalinization (xylene, 95682, Sigma-Aldrich, St. Louis, MO, USA) and paraffinization (1496904, Sigma-Aldrich, St. Louis, MO, USA). Following dewaxing and rehydration, 5-μm sections were trimmed from the paraffin-embedded tissues and then subjected to hematoxylin-eosin (HE) staining. In short, the sections were stained utilizing hematoxylin (HY-N0116, MedChemExpress, Monmouth Junction, NJ, USA) for 8 min, differentiated using 1% hydrochloric alcohol, treated with slightly alkaline water (67362, Sigma-Aldrich, St. Louis, MO, USA) for developing blue coloration, and finally dyed with eosin (E91810, ACMEC biotechemical, Shanghai, China) for 5 min. Then, after sealing with neutral balsam (N861409, Macklin, Shanghai, China), an optical microscope (×100 magnification; ZEISS Primotech, Carl Zeiss, Oberkochen, Germany) was employed to observe the staining results. Subsequently, the area/total area of pulmonary artery (WA/TA) in the left pulmonary tissues was calculated.

Terminal Deoxynucleotidyl Transferase-Mediated dUTP Nick-End Labeling Assay

Apoptosis of artery endothelial cells in the left pulmonary artery tissue sections, which had been stained by hematoxylin and eosin, was assessed with terminal deoxynucleotidyl transferase-mediated dUTP nick-end labeling (TUNEL) assay kit (C1098, Beyotime, Shanghai, China). Briefly, the sections were probed with proteinase K (ST533, Beyotime, Shanghai, China) (room temperature, 30 min) and with H_2O_2 (20 min). Subsequently, treatment of tissue sections with biotin-labeled terminal deoxynucleotidyl transferase (TdT) incubation buffer (37 °C, 10 min) and streptavidin-horseradish peroxidase (HRP) working solution (30 min) was performed, followed by color development using diaminobenzidine (DAB) solution and counterstaining using hematoxylin. The brown part in the stained section indicates the positively stained cells. TUNEL-positive cells were enumerated using a confocal microscopy (LEXT OLS5100, Olympus, Tokyo, Japan) under ×100 magnification. The relative positive area rate was calculated using the formula given in the following:

Relative positive area rate (%) = TUNEL positive area/total area × 100%.

Immunohistochemistry

The preprocessed left pulmonary artery tissues were treated with sodium citrate-hydrochloric acid buffer, boiled to retrieve antigen, and then treated with H_2O_2 for 20 min. After blocking with bovine serum albumin (BSA; A1933, 5%, Sigma-Aldrich, St. Louis, MO, USA) for 2 h, the sections were incubated with antibodies against mTORC1 (ab32028, Abcam, London, UK), ATF4 (MA5-32364, ThermoFisher, Waltham, MA, USA), and MCP-1 (ab7202, Abcam, London, UK) at 4 °C overnight, and then with secondary antibody goat anti-rabbit IgG (31460, ThermoFisher, Waltham, MA, USA) for 20 min. Later, color was developed by treating the sections with DAB solution (11718096001, Sigma-Aldrich, St. Louis, MO, USA) for 2 min, and hematoxylin was utilized for counterstaining. The brown part on the section indicates the positively stained cells. Areas positive for mTOR, ATF4 and MCP-1 were microscopically observed under ×100 magnification, and the positive areas of mTOR, ATF4 and MCP-1 were analyzed using ImageJ software (1.52s version, National Institutes of Health, Bethesda, MA, USA) to measure their expressions in the rat pulmonary artery tissues.

Isolation and Culture of Rat Pulmonary Artery Endothelial Cells

Rat pulmonary artery endothelial cells (RPAECs) were prepared from pulmonary artery tissues of CTEPH rat, which had been subjected to collagenase incubation, as reported previously [24]. In short, confluent RPAECs were digested with trypsin-ethylenediaminetetraacetic acid (EDTA) (T4049, Sigma-Aldrich, St. Louis, MO, USA) and propagated in DMEM (A4192101, ThermoFisher, Waltham, MA, USA) supplemented with 10% horse serum (SR0035C, ThermoFisher, Waltham, MA, USA), 5% fetal bovine serum (FBS; 30067334, ThermoFisher, Waltham, MA, USA), 100 μg/mL endothelial cell growth supplement (213-GS, Sigma-Aldrich, St. Louis, MO, USA), 20 mmol/L HEPES (11344041, ThermoFisher, Waltham, MA, USA), 2 mmol/L glutamine (21051040, ThermoFisher, Waltham, MA, USA), and 50 IU/mL-50 μg/mL penicillin-streptomycin (15070063, ThermoFisher, Waltham, MA, USA). A humidified chamber (5% CO_2, 37 °C) was employed for cell culture, and cells from passage 2 were used in this study. RPAECs were routinely subjected to mycoplasma contamination test and were confirmed to be mycoplasma-free.

Journal of
BIOLOGICAL REGULATORS
and Homeostatic Agents

Identification of RPAECs

Immunofluorescence was performed for cell identification. CTEPH RPAECs were subjected to 10-min fixation (4% paraformaldehyde), 20-min detachment (0.5% Triton X-100, X100, Sigma-Aldrich, St. Louis, MO, USA), and 30-min blocking (BSA). The blocked cells were cultured with CD31 (MA1-80069, ThermoFisher, Waltham, MA, USA) and von Willebrand Factor (vWF) (MA5-42805, ThermoFisher, Waltham, MA, USA) antibodies at 4 °C overnight, and with red fluorescence-labeled Dil-labeled acetylated low density lipoprotein (Dil-Ac-LDL) (synthesized by maokangbio; Shanghai, China) at 37 °C for 2 h. Subsequently, further incubation of cells with Alexa Fluor 514-conjugated goat anti-mouse and goat anti-rabbit (A-31555, A-11034, ThermoFisher, Waltham, MA, USA) antibodies at room temperature for 1 h was conducted. Nuclei were stained utilizing 4′,6-diamidino-2-phenylindole (DAPI; C1002, Beyotime, Shanghai, China). Lastly, positive cells were microscopically observed under ×200 magnification.

Cell Transfection

The coding sequence (CDS) region of the *ATF4* gene (**Supplementary material**) was inserted into the pcDNA3.1 vector (V79520, ThermoFisher, Waltham, MA, USA) to construct ATF4 overexpression plasmid, and an empty vector was employed as the negative control (NC). CTEPH RPAECs were transfected with ATF4 overexpression plasmid or NC using Lipofectamine 3000 transfection reagent (L3000015, ThermoFisher, Waltham, MA, USA). Briefly, CTEPH RPAECs in 96-well plates (1×10^4/well) were cultured until 80% confluent and then incubated with gene-lipid complexes obtained from the incubation of the above plasmids with Lipofectamine 3000 reagent. The cell incubation was conducted for 8 h at 37 °C for transfection.

AZD8055 Treatment

To determine the involvement of mTORC1 during CTEPH progression, CTEPH RPAECs were plated and grown to 80% confluence in 60-mm dishes prior to serum-deprivation for 24 h. Following serum deprivation, CTEPH RPAECs were treated with 250 nmol/L AZD8055 dissolved in DMSO in serum-deprived medium at 37 °C for 24 h [25].

Western Blotting

The concentration of total proteins from pulmonary artery tissues, as well as CTEPH RPAECs which had undergone transfection and/or AZD8055 treatment using radioimmunoprecipitation assay (RIPA) buffer (HC1237, BIOFOUNT, Beijing, China), was determined using BCA kits (A53227, ThermoFisher, Waltham, MA, USA). The protein was loaded, separated on NuPAGE Bis-Tris gel (NP0326BOX, ThermoFisher, Waltham, MA, USA), and then placed onto polyvinylidene fluoride membranes (P2438, Sigma-Aldrich, St. Louis, MO, USA). After being blocked with 5% non-fat milk at room temperature for 2 h in Tris-buffered saline with 1% Tween 20 (TBST, TA-125-TT, ThermoFisher, Waltham, MA, USA), the membranes were incubated at 4 °C overnight with primary antibodies, mTORC1 (#2972, 289 kDa, 1:1000) and ATF4 (#11815, 49 kDa, 1:1000) acquired from Cell Signaling Technology (Danvers, MA, USA), as well as MCP-1 (ab7202, 18 kDa, 1:2000) and glyceraldehyde-3-phosphate dehydrogenase (GAPDH) (ab8245, 36 kDa, 1:500) from Abcam (London, UK). Later, after washing with TBST thrice, incubation of the membranes with secondary antibodies goat anti-rabbit/mouse IgG (31460/PA1-28568, 1:10,000, ThermoFisher, Waltham, MA, USA) was performed at room temperature for 1 h. Immunoblot visualization was conducted using ECL reagent kits (ab133409, Abcam, London, UK) on an imager (Tanon-2500, Tanon, Shanghai, China), and densitometric analysis was performed using ImageJ software (1.52s version, National Institutes of Health, Bethesda, MA, USA). The normalized relative protein expression level was calculated using the formula below:

x′ (normalized data) = (x (original data) – mean data (x))/std data (x, internal control).

Cell Counting Kit-8 Assay

The transfected CTEPH RPAECs in 96-well plates (2×10^3/well) underwent AZD8055 treatment or not. After being cultured with 100 μL specific culture medium to be adherent to the plate, the cells were added with 10 μL cell counting kit-8 (CCK-8) reagent (C0037, Beyotime, Shanghai, China). Cell incubation was conducted at 37 °C for 2 h, followed by cell absorbance measurement (450 nm) using a microplate reader (GM2010, Promega, Madison, WI, USA).

Flow Cytometry

CTEPH RPAECs at 5×10^6 cells/100 μL were acquired through digestion with EDTA-deprived trypsin (T2600000, 0.25%, Sigma-Aldrich, St. Louis, MO, USA) and suspension with phosphate-buffered saline (PBS; P3813, Sigma-Aldrich, St. Louis, MO, USA). The cell suspension was stained with APC-conjugated antibody against CD31 (ab275710, Abcam, London, UK) at 4 °C for 30 min in the dark.

CTEPH RPAECs which had been transfected and/or treated with AZD8055 were subjected to apoptosis determination using Annexin V-fluorescein isothiocyanate (FITC)/PI Apoptosis Double Staining kits (556547, Livning, Beijing, China). Next, the cells were digested with 0.25% EDTA-deprived trypsin, centrifuged (2000 ×g, 10 min) and then resuspended in binding buffer, after which cell staining was conducted using Annexin V-FITC (5 μL, 15 min) and propidium iodide (PI; 5 μL, 5 min) in the dark.

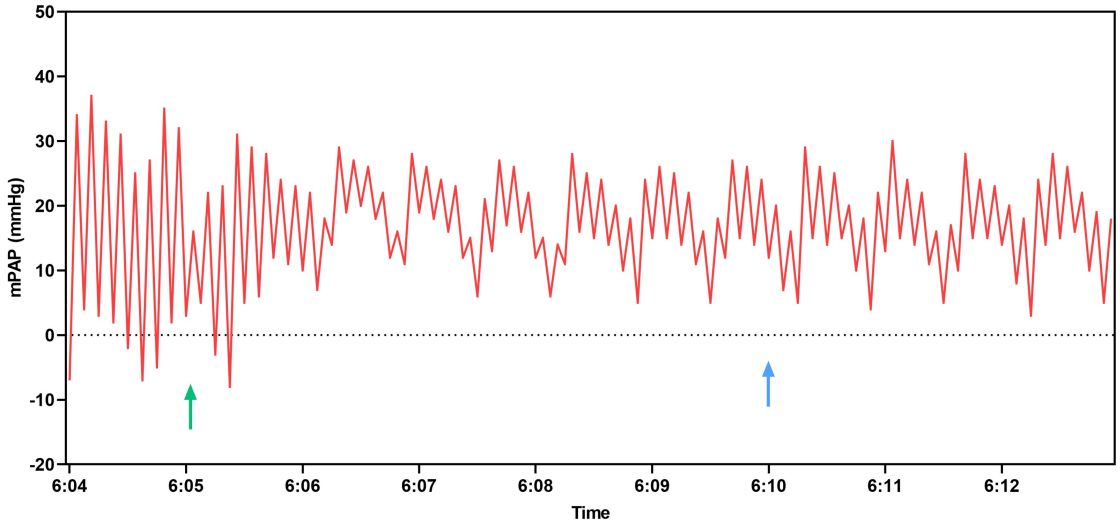

Fig. 1. Waveform curves for the RVP and mPAP of CTEPH rats. RVP is indicated by green arrow, and mPAP is indicated by blue arrow. CTEPH, chronic thromboembolic pulmonary hypertension; RVP, right ventricular pressure; mPAP, mean pulmonary artery pressure.

The stained cell suspension was loaded into a flow cytometer (Cytoflex, Beckman Coulter, Brea, CA, USA) for endothelial cell identification and apoptosis analysis.

Quantitative Reverse Transcription Polymerase Chain Reaction

Total RNA from CTEPH RPAECs which had been transfected and/or treated with AZD8055 was isolated using RNAiso Plus reagent (9109, TaKaRa, Tokyo, Japan), and reverse-transcribed into complementary DNA (cDNA) using iScript cDNA Synthesis kits (11483188001, Sigma-Aldrich, St. Louis, MO, USA). The cDNA was amplified via real-time polymerase chain reaction (PCR) on a system (Gradient Thermal Cycler, BioRad Lab., Hercules, CA, USA) with Green Premix Ex Taq (RR420Q, TaKaRa, Tokyo, Japan). The thermal cycling conditions were set as follows: 95 °C for 10 min, followed by 40 cycles of 95 °C for 15 s, and 60 °C for 1 min. Primers used in the reaction include those for *MCP-1* and *GAPDH*, with sequences given in the following: *MCP-1*, (forward) 5′-CCACTCACCTGCTGCTACTC-3′ and (reverse) 5′-ACCTGCTGCTGGTGATTCTC-3′; *GAPDH*, (forward) 5′-GCGAGATCCCGCTAACATCA-3′ and (reverse) 5′-ATTCGAGAGAAGGGAGGGCT-3′. The relative *MCP-1* expression was calculated using the $2^{-\Delta\Delta Ct}$ method [26] and normalized against the *GAPDH* expression.

Enzyme-Linked Immunosorbent Assay

CTEPH RPAECs that had been transfected and/or treated with AZD8055 were centrifuged (1000 ×g, 37 °C, 10 min) to obtain supernatant. Enzyme-linked immunosorbent assay (ELISA) kits (ml002960, mlbio, Shanghai, China) were utilized to assess the secretion of MCP-1 from the cell supernatant. Briefly, enzyme-coated plates were incubated with the supernatant (50 µL) (37 °C, 30 min), and then with biotinylated antibodies (50 µL) (37 °C, 30 min), after which HRP-conjugated enzyme (80 µL) was used for another 30-min incubation at 37 °C. Color development was preformed via incubation with A substrate (50 µL) and B substrate (50 µL) for 10 min. Following reaction termination triggered by stop solution, absorbance was read at 450 nm using a microplate reader.

Bioinformatics Analysis

The motiflogo map of ATF4 and binding sites for ATF4 on the sequence of *MCP-1* were analyzed on the JASPAR website (http://jaspar.genereg.net/analysis).

Chromatin Immunoprecipitation Assay

After being transfected with wild-type/mutant-type or ATF4 overexpression plasmid, CTEPH RPAECs (70–80% confluence) were collected and fixed with 1% formaldehyde (room temperature, 10 min) for promoting DNA-protein crosslinking. After the reaction was terminated by glycine, the sample was lysed by RIPA buffer, sonicated by ultrasonic treatment, and centrifuged (10,000 ×g, 4 °C). Later, the sample was incubated with RNA polymerase II or the antibody against IgG, ATF4 (#11815, Cell signaling technology, Danvers, MA, USA) or MCP-1 (MAB2137, R&D Systems, Minneapolis, MN, USA) at 4 °C overnight. Precipitation of DNA-protein complex was then induced by protein agarose (20334, ThermoFisher, Waltham, MA, USA). The non-specific complexes were washed and decrosslinked at 65 °C. After being purified and recovered by phenol/chloroform, the DNA fragments were subjected to

Journal of
BIOLOGICAL REGULATORS
and Homeostatic Agents

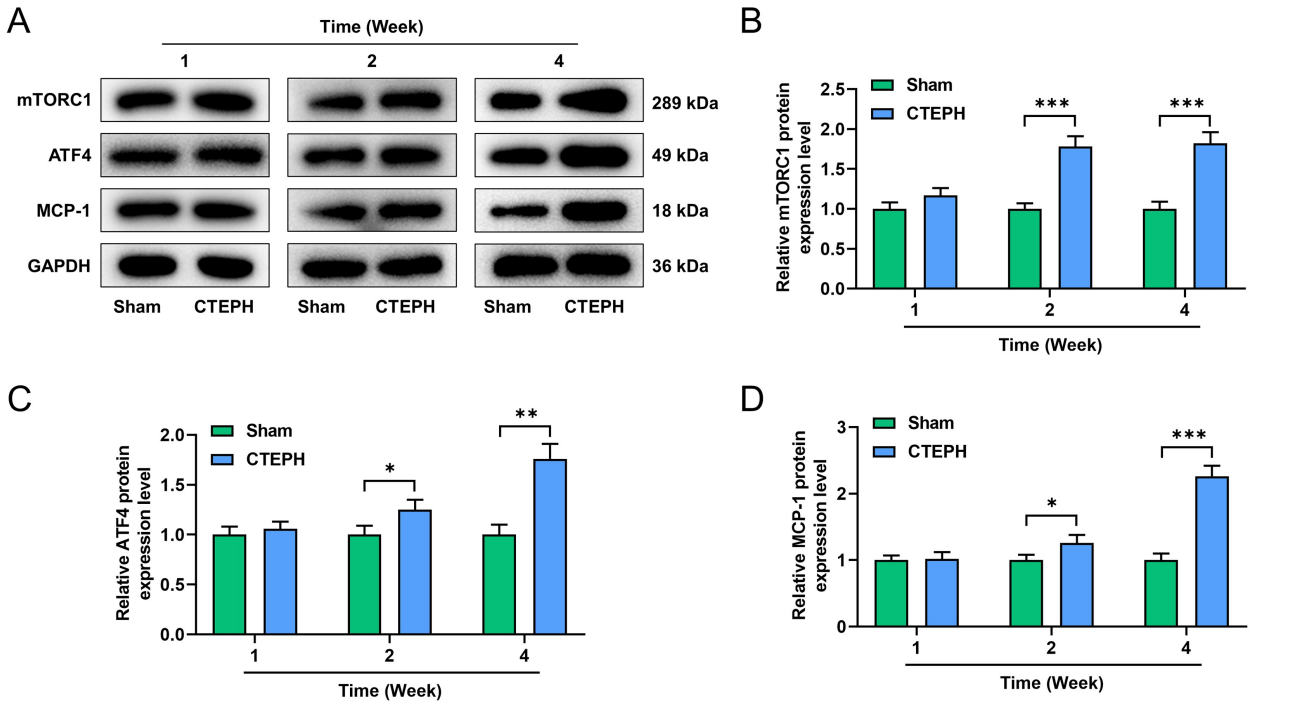

Fig. 2. The mTORC1-ATF4-MCP-1 pathway was activated in pulmonary artery tissues of CTEPH rats. (A–D) The expression of mTORC1, ATF4 and MCP-1 in the pulmonary artery tissues of rats at the 1st, 2nd and 4th week after CTEPH induction was analyzed by means of Western blotting, with GAPDH serving as the internal control. N = 3; * $p < 0.05$; ** $p < 0.01$; *** $p < 0.001$. CTEPH, chronic thromboembolic pulmonary hypertension; mTORC1, mammalian target of rapamycin complex 1; ATF4, activating transcription factor 4; MCP-1, monocyte chemoattractant protein-1; GAPDH, glyceraldehyde-3-phosphate dehydrogenase.

quantitative reverse transcription polymerase chain reaction (qRT-PCR) to detect the enrichment of ATF4 in the MCP-1 promoter region.

Statistical Analyses

Statistical analyses were conducted using GraphPad prism (version 8.0, GraphPad Software Inc., San Diego, CA, USA). All data are expressed as mean ± standard deviation (SD). Two-group differences were analyzed using independent *t*-tests, while multi-groups differences were evaluated by one-way analysis of variance (ANOVA). Differences with $p < 0.05$ were considered statistically significant.

Results

The mTOR-ATF4-MCP-1 Pathway was Activated in Pulmonary Artery Tissues of CTEPH Rats

Measurements of RVP and mPAP were conducted to determine the success of modeling CTEPH in rat. The results showed that the RVP and mPAP were increased after CTEPH modeling (Fig. 1). Next, through Western blotting, the status of in the lung tissues was tested. We found that the expression of mTORC1, ATF4 and MCP-1—the key players in the mTOR-ATF4-MCP-1 pathway—was increased in the lung tissues of rats at the 2nd and 4th week after the first pulmonary emboli appeared in the rats ($p < 0.05$, Fig. 2A–D).

AZD8055 Lowered mPAP and Inhibited Pulmonary Thromboembolism in CTEPH Rats

AZD8055, an mTORCR1 inhibitor, was employed to assess whether the mTOR-ATF4-MCP-1 pathway was engaged in the development of CTEPH. Injection of AZD8055 decreased the mPAP of CTEPH rats, compared to DMSO injection (Fig. 3A, $p < 0.05$). Meanwhile, through naked-eye observation and hematoxylin-eosin staining, CTEPH rats, in comparison to the Sham rats, were observed to exhibit apparent pulmonary thromboembolism, which could be alleviated by AZD8055 injection relative to DMSO injection (Fig. 3B,C). The WA/TA was augmented in rats after CTEPH induction (Fig. 3D, $p < 0.001$), but AZD8055 injection offset the CTEPH-related WA/TA increase in rats, compared to DMSO injection (Fig. 3D, $p < 0.01$). Besides, the CTEPH-induced up-regulated expression of mTORC1, ATF4 and MCP-1 in the rat lung tissues was attenuated following AZD8055 injection (Fig. 3E, $p < 0.001$).

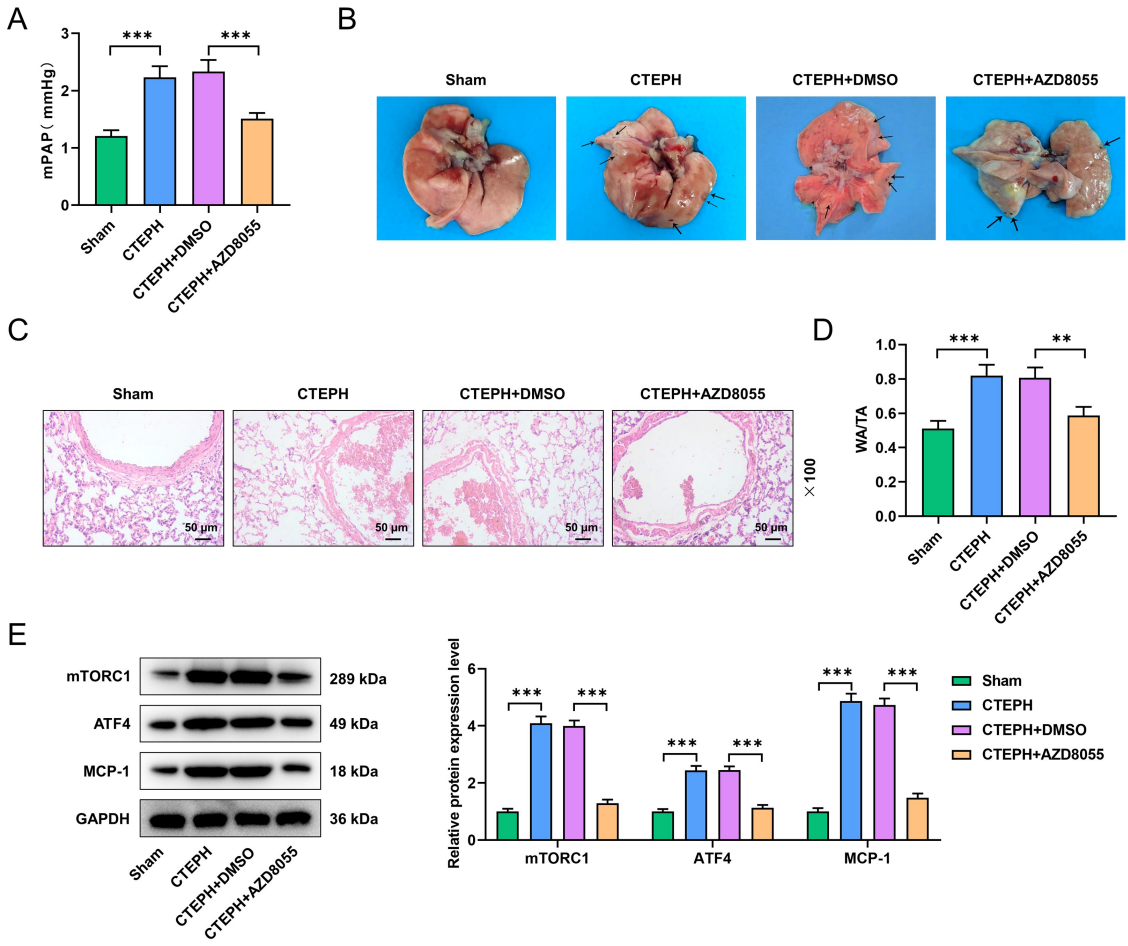

Fig. 3. AZD8055 lowered mPAP and inhibited pulmonary thromboembolism in CTEPH rats. (A) The mPAP of CTEPH rats treated with DMSO/AZD8055 was measured by a murine non-invasive blood pressure monitor. (B,C) The thromboembolism and other pathological conditions of the pulmonary tissues of CTEPH rats treated with DMSO/AZD8055 were examined with naked eyes (B) and confirmed with hematoxylin-eosin staining (scale bar: 50 μm, magnification: ×100) (C). The black arrow indicates thromboembolism. (D) The WA/TA of CTEPH rats treated with DMSO/AZD8055 was calculated. (E) The expression of mTOR, ATF4 and MCP-1 in the pulmonary artery tissues of CTEPH rats treated with DMSO/AZD8055 were analyzed by Western blotting, with GAPDH serving as the internal control. N = 3; ** $p < 0.01$, *** $p < 0.001$. CTEPH, chronic thromboembolic pulmonary hypertension; mPAP, mean pulmonary artery pressure; WA/TA, area/total area of pulmonary artery; mTORC1, mammalian target of rapamycin complex 1; ATF4, activating transcription factor 4; MCP-1, monocyte chemoattractant protein-1; DMSO, dimethyl sulfoxide.

AZD8055 Blocked Cell Apoptosis and Suppressed the mTORC1-ATF4-MCP-1 Pathway in Pulmonary Artery Tissues of CTEPH Rats

CTEPH rats possessed more TUNEL-positive apoptotic cells in the pulmonary artery tissues, compared to the Sham rats (Fig. 4A, $p < 0.05$), but AZD8055 injection, in contrast to DMSO injection, could reverse the increase of the apoptotic cell number (Fig. 4A, $p < 0.01$). Meanwhile, immunohistochemistry assay revealed that the area positive for mTORC1, ATF4 or MCP-1 in the pulmonary artery tissues of rats was found to be increased after CTEPH induction (Fig. 4B, $p < 0.001$), and the increase was offset by AZD8055 injection relative to DMSO injection (Fig. 4B, $p < 0.05$).

AZD8055-Induced mTORC1-ATF4-MCP-1 Pathway Suppression, Viability Increase, and Apoptosis Inhibition in CTEPH RPAECs were Reversed by ATF4 Overexpression

RPAECs isolated from CTEPH rats were experimentally utilized to verify the effect of mTOR-ATF4-MCP-1 pathway on endothelial cell disorders. CD31-positive cells expressing CD31, vWF and Dil-Ac-LDL were identified as RPAECs through immunofluorescence assay (Fig. 5A) and flow cytometry (Fig. 5B), respectively.

Subsequently, we treated the isolated RPAECs (CTEPH RPAECs) with AZD8055. AZD8055 application lessened the expression of mTOR, ATF4 and MCP-1 in the CTEPH RPAECs (Fig. 5C, $p < 0.01$). ATF4 was over-

Journal of
BIOLOGICAL REGULATORS
and Homeostatic Agents

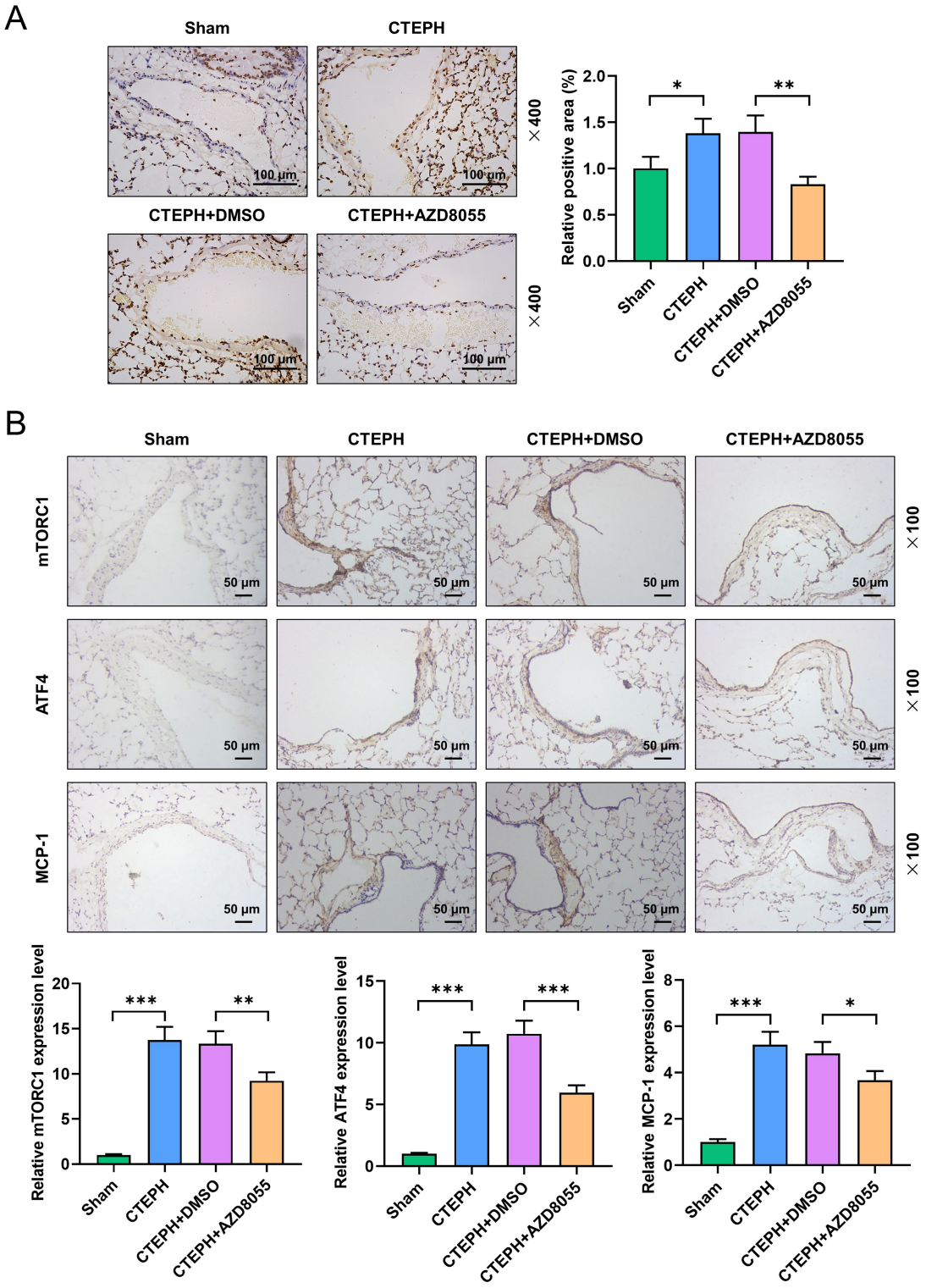

Fig. 4. AZD8055 inhibited cell apoptosis and suppressed the mTORC1-ATF4-MCP-1 pathway in pulmonary artery tissues of CTEPH rats. (A) The cell apoptosis in the pulmonary artery tissues of CTEPH rats treated with DMSO/AZD8055 was assessed by TUNEL assay (scale bar: 100 μm, magnification: ×400); the brown part indicates positive cells. (B) The expression of mTOR, ATF4 and MCP-1 in the pulmonary artery tissues of CTEPH rats treated with DMSO/AZD8055 was determined by immunohistochemistry (scale bar: 50 μm, magnification: ×100). N = 3; * $p < 0.05$, ** $p < 0.01$, *** $p < 0.001$. CTEPH, chronic thromboembolic pulmonary hypertension; mTORC1, mammalian target of rapamycin complex 1; ATF4, activating transcription factor 4; MCP-1, monocyte chemoattractant protein-1; DMSO, dimethyl sulfoxide.

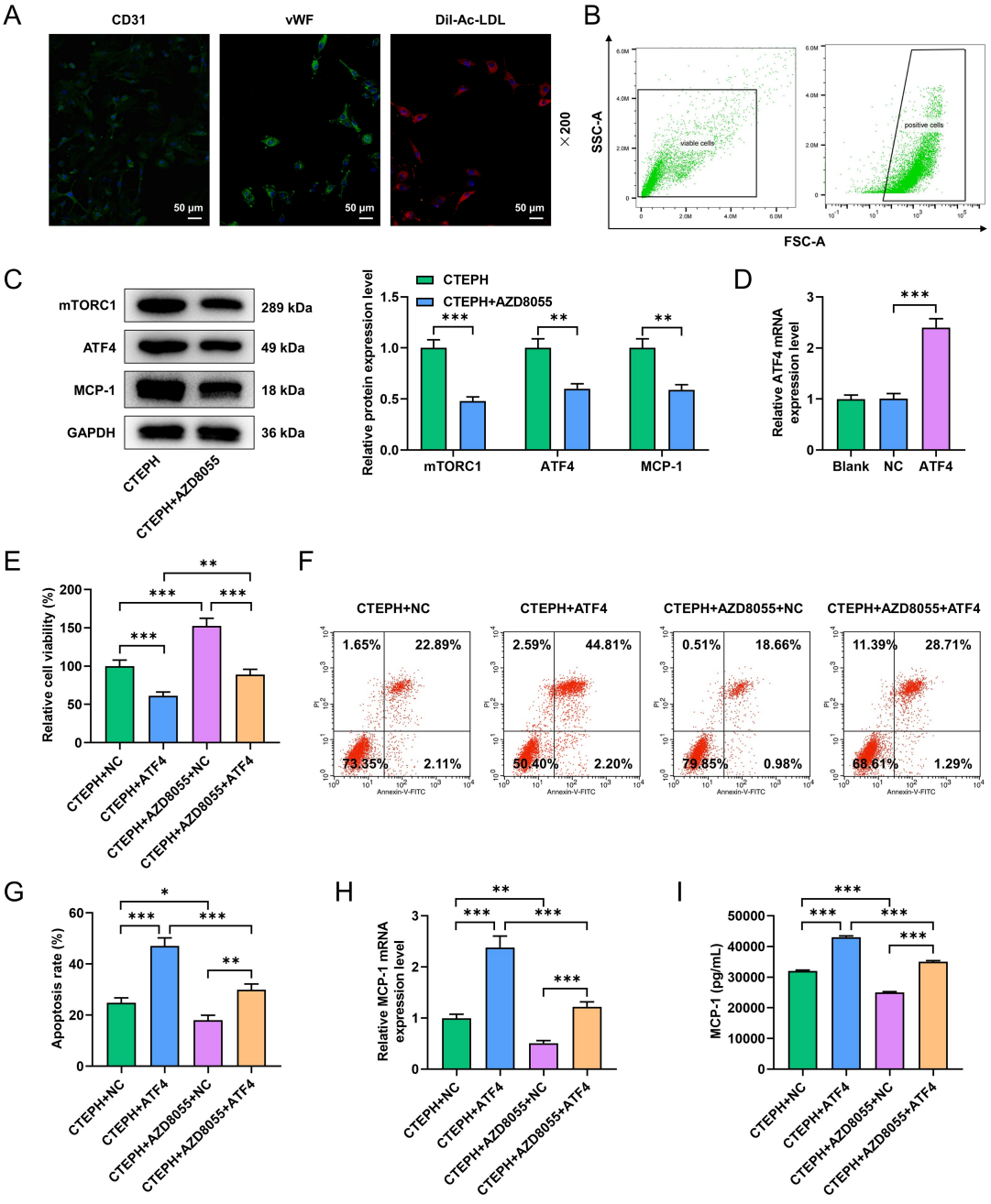

Fig. 5. AZD8055-induced mTORC1-ATF4-MCP-1 pathway suppression, viability increase, and apoptosis inhibition in CTEPH RPAECs were reversed by ATF4 overexpression. (A,B) RPAECs were isolated and identified by immunofluorescence (scale bar: 50 μm, magnification: ×200) (A) and flow cytometry (B). (C) The expression of mTOR, ATF4 and MCP-1 in CTEPH RPAECs treated with AZD8055 were analyzed by means of Western blotting, with GAPDH serving as the internal control. (D) The transfection efficiency of ATF4 overexpression plasmid in CTEPH rat pulmonary artery endothelial cells was evaluated by qRT-PCR, with GAPDH serving as the internal control. (E) The viability of CTEPH RPAECs transfected with ATF4 overexpression plasmid and treated with AZD8055 was measured by cell counting kit-8 (CCK-8) assay. (F,G) The apoptosis of CTEPH rat pulmonary artery endothelial cells transfected with ATF4 overexpression plasmid and treated with AZD8055 was determined by flow cytometry. (H,I) The expression or secretion of MCP-1 in or from CTEPH RPAECs transfected with ATF4 overexpression plasmid and treated with AZD8055 was analyzed by qRT-PCR, with GAPDH serving as the internal control (H), or by enzyme-linked immunosorbent assay (I). N = 3; * $p < 0.05$, ** $p < 0.01$, *** $p < 0.001$. CTEPH, chronic thromboembolic pulmonary hypertension; mTORC1, mammalian target of rapamycin complex 1; ATF4, activating transcription factor 4; MCP-1, monocyte chemoattractant protein-1; NC, negative control; RPAECs, rat pulmonary artery endothelial cells; vWF, von Willebrand Factor; Dil-Ac-LDL, Dil-labeled acetylated low density lipoprotein.

Journal of
BIOLOGICAL REGULATORS
and Homeostatic Agents

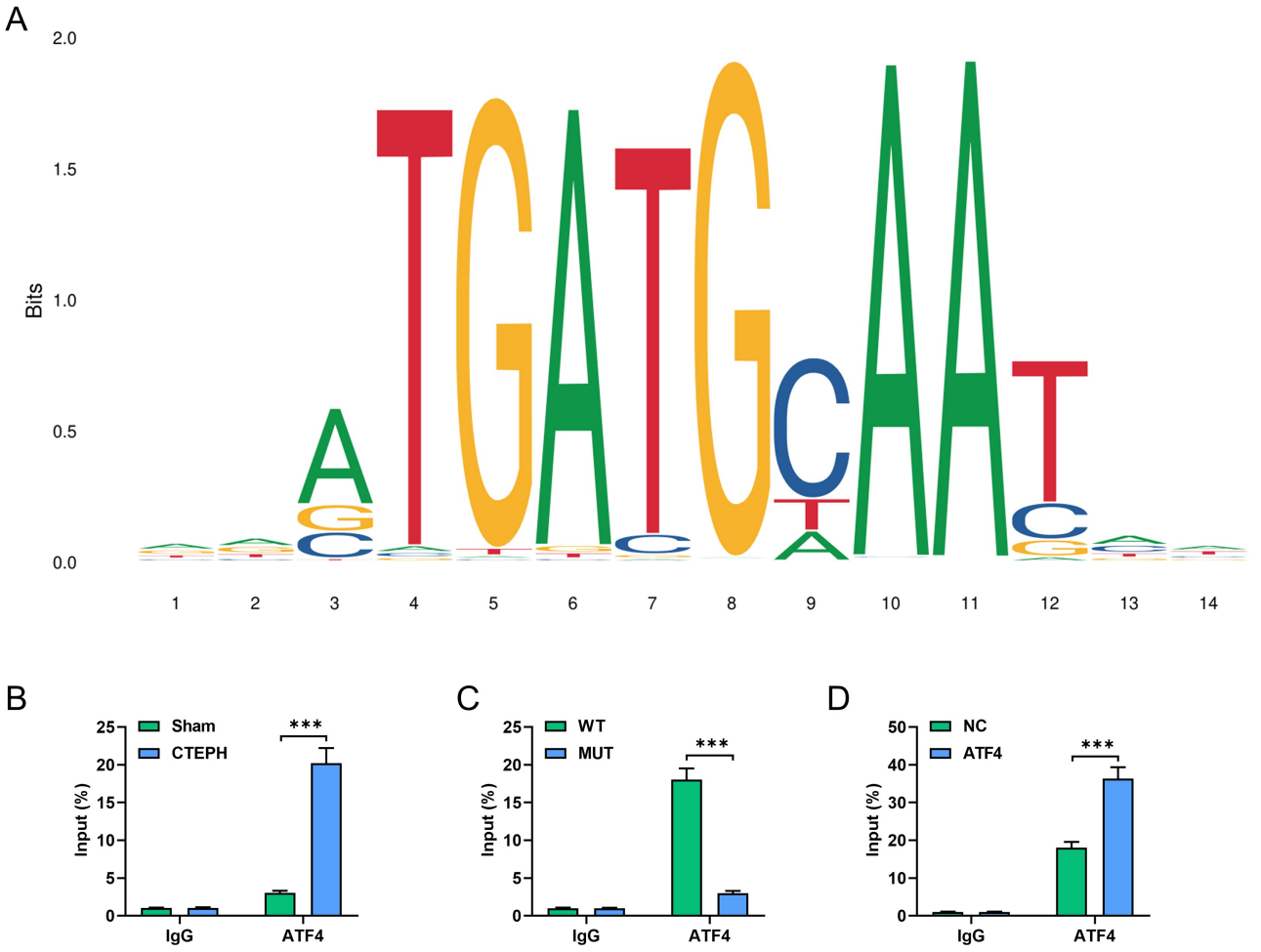

Fig. 6. ATF4 transcriptionally upregulated MCP-1 expression in CTEPH RPAECs. (A–D) The interaction between ATF4 and MCP-1 was predicted by analyses performed on the JASPAR website (A) and validated through ChIP assay in CTEPH RPAECs (B–D). N = 3; *** $p < 0.001$. ATF4, activating transcription factor 4; ChIP, Chromatin immunoprecipitation; MCP-1, monocyte chemoattractant protein-1; MUT, mutant-type, NC, negative control; RPAECs, rat pulmonary artery endothelial cells; WT, wild-type.

expressed in the RPAECs via transfection (Fig. 5D, $p < 0.001$). ATF4 overexpression plasmid transfection, compared to NC transfection, resulted in decreased viability of the CTEPH RPAECs (Fig. 5E, $p < 0.001$). Conversely, the CTEPH RPAEC viability was enhanced by AZD8055 application (Fig. 5E, $p < 0.001$). When used together, however, AZD8055 application and ATF4 overexpression mutually negated their effects on the viability of CTEPH RPAECs (Fig. 5E, $p < 0.01$). In the meantime, the apoptosis of CTEPH RPAECs was elevated after ATF4 overexpression plasmid transfection relative to NC transfection (Fig. 5F,G, $p < 0.001$), but AZD8055 application prevented the apoptosis of CTEPH RPAECs (Fig. 5F,G, $p < 0.05$). Similarly, AZD8055 application and ATF4 overexpression mutually offset their effects on the apoptosis of CTEPH RPAECs (Fig. 5F,G, $p < 0.01$). Moreover, compared to NC transfection, ATF4 overexpression plasmid transfection led to upregulation of MCP-1 in CTEPH RPAECs (Fig. 5H,I, $p < 0.001$); on the contrary, AZD8055 application diminished the expression of MCP-1 (Fig. 5H,I, $p < 0.01$). In other words, ATF4 overexpression and AZD8055 application mutually negate their effects on the expression of ATF4 in CTEPH RPAECs (Fig. 5H,I, $p < 0.001$).

ATF4 Transcriptionally Upregulated MCP-1 Expression in CTEPH RPAECs

Analyses conducted on the JASPAR website led to the generation of a motif map of ATF4 (Fig. 6A). Chromatin immunoprecipitation (ChIP) was then performed to dissect the interaction between ATF4 and MCP-1. As presented in Fig. 6B, ATF4 was enriched in the MCP-1 promoter region in CTEPH RPAECs incubated with anti-ATF4 antibody, compared to that in CTEPH RPAECs cultured with IgG ($p < 0.001$). When the wild-type binding sites were mutated in CTEPH RPAECs, the ATF4 enrichment in the MCP-1 promoter region was prominently reduced (Fig. 6C, $p < 0.001$). ATF4 overexpression plasmid transfection could bring about more enrichment of ATF4 in the MCP-1 pro-

moter region in CTEPH RPAECs, as compared to NC transfection (Fig. 6D, $p < 0.001$). These results collectively indicated that ATF4 can bind to the MCP-1 promoter region and induce MCP-1 expression in CTEPH.

Discussion

CTEPH occurs as a result of recurrent or incomplete treatment of acute PE induced by thromboembolic material [27], with an incidence rate of 2.3% among survivors of acute PE [1]. CTEPH is characterized by the chronic arterial obstruction visible at macroscopic level and the resulting vascular remodeling in the microvasculature of the pulmonary system [28]. These pathological events are driven by endothelial dysfunction-induced disorganization of the vascular wall and subsequent vascular lesions [29]. mTOR is a nutrient/energy/redox sensor, whose contribution to CTEPH progression through promoting vascular remodeling has been documented [12]. This study unveiled that the activation of the mTORC1-ATF4-MCP-1 pathway serves as the mechanism underlying CTEPH progression by inducing endothelial dysfunction.

mTOR can be activated by thrombin and contribute to pulmonary vascular remodeling in pulmonary hypertension [30]. mTORC1 has been shown to promote aging-related venous thrombosis [31] and play a causative role in pulmonary arterial hypertension [13]. In the present study, the autologous thromboembolization was repeatedly triggered in rats to induce CTEPH, which was confirmed to be successful by measuring the RVP and mPAP of the rats. We discovered that mTORC1, ATF4 and MCP-1 expression was upregulated at week 2 and 4 post CTEPH induction. These results, combined with previous findings that mTORC1 mediates ATF4 activation [18] and ATF4 can positively regulate MCP-1 in endothelial cells [21], imply that the activation of the mTORC1-ATF4-MCP-1 pathway is a potential driver of the development of CTEPH.

A physical examination of CTEPH patients has revealed that right ventricular impulse is a discernable sign of pulmonary arterial hypertension [32]. Consistent with this and the observation on CTEPH rat established previously [33], the rats in the present study were found to have elevated the RVP and mPAP levels after CTEPH induction. CTEPH is induced by pulmonary artery thromboembolism, which provokes chronic obstruction and pulmonary artery enlargement [34,35]. According to Zeng *et al.*'s study [22], rat models of CTEPH present an increased WA/TA, which is also observed in our CTEPH rats. In addition, although endothelial cells isolated via pulmonary endarterectomy from human patients with CTEPH displayed decreased apoptosis [36], Deng *et al.* [37] reported that apoptosis is induced in pulmonary artery endothelial cells during the four-week period of CTEPH development. Consistent with their results, our study revealed that the TUNEL-positive pulmonary artery endothelial cells were overrepresented in CTEPH rats, as compared to Sham rats. Notably, in the current study, all the above-mentioned pathological conditions occurred in the CTEPH rats, suggesting mTORC1-ATF4-MCP-1 pathway activation in the pulmonary artery tissues of CTEPH rats. Previous evidence reflected that mTOR inhibition confers potential therapeutic benefit on CTEPH by virtue of its ability to suppress vascular remodeling and reduce pulmonary vascular resistance [12,38,39]. In this study, inhibition of mTORC1 by AZD8055 injection was performed in CTEPH rats. Later, we observed that mTORC1 inhibition not only lowered the mPAP level and alleviated pulmonary artery thromboembolism, but also inhibited apoptosis of pulmonary artery endothelial cells and downregulated ATF4 and MCP-1 in CTEPH rat pulmonary artery tissues. These observations mirrored that mTORC1 inhibition suppressed CTEPH through attenuation of endothelial dysfunction and pulmonary artery thromboembolism, possibly mediated by downregulation of ATF4 and MCP-1 expression. However, the downstream signaling of mTORC1 has not been delineated yet, and this gap will be addressed in our future study.

To validate our postulation, *in vitro* experimentation was conducted with CTEPH pulmonary artery endothelial cells. Endoplasmic reticulum (ER) stress and protein folding inhibition, both of which lead to homocysteine-induced endothelial dysfunction, involve ATF4 upregulation [16]. The fact that ER stress, which is preceded by ATF4 upregulation for restoring cell homeostasis, can result in cell death if not reversed [40], provides links between ATF4 upregulation and cell death. Concurring with this finding, we found that overexpression of ATF4 reduced cell viability, increased apoptosis of CTEPH pulmonary artery endothelial cells, and weakened mTORC1 inhibition-induced protection for the cells in CTEPH context. Furthermore, as proposed previously, ATF4 induces the secretion of MCP-1 [21]. The mechanism underlying this finding was uncovered in our study, which revealed that ATF4 acts as a transcription factor to increase MCP-1 expression. Meanwhile, we observed that mTORC1 inhibition caused downregulation of MCP-1 expression in CTEPH pulmonary artery endothelial cells, which could be reversed by ATF4 overexpression. MCP-1 upregulation in the plasma is closely related to pulmonary vascular resistance in CTEPH [20]. CTEPH endothelial cells are in a basal pro-inflammatory status, which is reflected by increased production of inflammatory cytokines including MCP-1 and drives CTEPH progression [41]. Taken together, these findings point to the deleterious consequences of ATF4 overexpression to pulmonary artery endothelial cells in CTEPH through transcriptional upregulation of MCP-1 expression.

Conclusion

Collectively, this study demonstrated that activation of mTORC1-ATF4-MCP-1 pathway promotes CTEPH pro-

Journal of
BIOLOGICAL REGULATORS
and Homeostatic Agents

gression by inducing endothelial dysfunction and the ensuing pulmonary artery thromboembolism.

Availability of Data and Materials

The analyzed data sets generated during the study are available from the corresponding authors on reasonable request.

Author Contributions

Substantial contributions to conception and design: JYS, YL. Data acquisition, data analysis and interpretation: YYL, FPW, ZCX, KYS. Drafting the article or critically revising it for important intellectual content: All authors. Final approval of the version to be published: All authors. Agreement to be accountable for all aspects of the work in ensuring that questions related to the accuracy or integrity of the work are appropriately investigated and resolved: All authors.

Ethics Approval and Consent to Participate

In the premise of adherence to the guidelines of the Care and Use of Animals in Research and Teaching, and obtainment of ratification from the Ethics Committee of Zhejiang Baiyue Biotech Co., Ltd. for Experimental Animal Welfare (approval number: ZJBYLA-IACUC-20230309), all animal experiments were conducted.

Acknowledgment

Not applicable.

Funding

This work was supported by the Minhang District Science and Technology Commission [2020MHZ067 and 2019MHZ025]; the Minhang District Medical Education and Research Collaborative Health Service System for High-level Specialist Backbone Physicians Program [2020MZYS16].

Conflict of Interest

The authors declare no conflict of interest.

Supplementary Material

Supplementary material associated with this article can be found, in the online version, at https://doi.org/10.23812/j.biol.regul.homeost.agents.20243805.346.

References

[1] Papamatheakis DG, Poch DS, Fernandes TM, Kerr KM, Kim NH, Fedullo PF. Chronic Thromboembolic Pulmonary Hypertension: JACC Focus Seminar. Journal of the American College of Cardiology. 2020; 76: 2155–2169.

[2] Teerapuncharoen K, Bag R. Chronic Thromboembolic Pulmonary Hypertension. Lung. 2022; 200: 283–299.

[3] Nukala SB, Tura-Ceide O, Aldini G, Smolders VFED, Blanco I, Peinado VI, *et al*. Protein network analyses of pulmonary endothelial cells in chronic thromboembolic pulmonary hypertension. Scientific Reports. 2021; 11: 5583.

[4] Opitz I, Kirschner MB. Molecular Research in Chronic Thromboembolic Pulmonary Hypertension. International Journal of Molecular Sciences. 2019; 20: 784.

[5] El-Tanani M, Nsairat H, Aljabali AA, Serrano-Aroca Á, Mishra V, Mishra Y, *et al*. Role of mammalian target of rapamycin (mTOR) signalling in oncogenesis. Life Sciences. 2023; 323: 121662.

[6] Panwar V, Singh A, Bhatt M, Tonk RK, Azizov S, Raza AS, *et al*. Multifaceted role of mTOR (mammalian target of rapamycin) signaling pathway in human health and disease. Signal Transduction and Targeted Therapy. 2023; 8: 375.

[7] Long JY, Wang XJ, Li XY, Kong XH, Yang G, Zhang D, *et al*. Spinal Microglia and Astrocytes: Two Key Players in Chronic Visceral Pain Pathogenesis. Neurochemical Research. 2022; 47: 545–551.

[8] Peng Y, Wang Y, Zhou C, Mei W, Zeng C. PI3K/Akt/mTOR Pathway and Its Role in Cancer Therapeutics: Are We Making Headway? Frontiers in Oncology. 2022; 12: 819128.

[9] Ma L, Zhang R, Li D, Qiao T, Guo X. Fluoride regulates chondrocyte proliferation and autophagy via PI3K/AKT/mTOR signaling pathway. Chemico-biological Interactions. 2021; 349: 109659.

[10] Ma H, Jiang S, Yuan Y, Li J, Li Y, Lv Y, *et al*. RUNX1 promotes proliferation and migration in non-small cell lung cancer cell lines via the mTOR pathway. FASEB Journal: Official Publication of the Federation of American Societies for Experimental Biology. 2023; 37: e23195.

[11] Szwed A, Kim E, Jacinto E. Regulation and metabolic functions of mTORC1 and mTORC2. Physiological Reviews. 2021; 101: 1371–1426.

[12] Ogawa A, Firth AL, Yao W, Madani MM, Kerr KM, Auger WR, *et al*. Inhibition of mTOR attenuates store-operated Ca2+ entry in cells from endarterectomized tissues of patients with chronic thromboembolic pulmonary hypertension. American Journal of Physiology. Lung Cellular and Molecular Physiology. 2009; 297: L666–L676.

[13] He Y, Zuo C, Jia D, Bai P, Kong D, Chen D, *et al*. Loss of DP1 Aggravates Vascular Remodeling in Pulmonary Arterial Hypertension via mTORC1 Signaling. American Journal of Respiratory and Critical Care Medicine. 2020; 201: 1263–1276.

[14] Reho JJ, Guo DF, Morgan DA, Rahmouni K. mTORC1 (Mechanistic Target of Rapamycin Complex 1) Signaling in Endothelial and Smooth Muscle Cells Is Required for Vascular Function. Hypertension (Dallas, Tex.: 1979). 2021; 77: 594–604.

[15] Mukherjee D, Bercz LS, Torok MA, Mace TA. Regulation of cellular immunity by activating transcription factor 4. Immunology Letters. 2020; 228: 24–34.

[16] Cheng CK, Luo JY, Lau CW, Cho WCS, Ng CF, Ma RCW, *et al*. A GLP-1 analog lowers ER stress and enhances protein folding to ameliorate homocysteine-induced endothelial dysfunction. Acta Pharmacologica Sinica. 2021; 42: 1598–1609.

[17] Ben-Sahra I, Hoxhaj G, Ricoult SJH, Asara JM, Manning BD. mTORC1 induces purine synthesis through control of the mitochondrial tetrahydrofolate cycle. Science (New York, N.Y.). 2016; 351: 728–733.

[18] Torrence ME, MacArthur MR, Hosios AM, Valvezan AJ, Asara JM, Mitchell JR, *et al*. The mTORC1-mediated activation of ATF4 promotes protein and glutathione synthesis downstream of growth signals. eLife. 2021; 10: e63326.

[19] Singh S, Anshita D, Ravichandiran V. MCP-1: Function, regulation, and involvement in disease. International Immunopharmacology. 2021; 101: 107598.
[20] Kimura H, Okada O, Tanabe N, Tanaka Y, Terai M, Takiguchi Y, *et al*. Plasma monocyte chemoattractant protein-1 and pulmonary vascular resistance in chronic thromboembolic pulmonary hypertension. American Journal of Respiratory and Critical Care Medicine. 2001; 164: 319–324.
[21] Huang H, Jing G, Wang JJ, Sheibani N, Zhang SX. ATF4 is a novel regulator of MCP-1 in microvascular endothelial cells. Journal of Inflammation (London, England). 2015; 12: 31.
[22] Zeng M, Chen S, Li H, Huang Z, Wu D, Pan Y, *et al*. The role of β-catenin in pulmonary artery endothelial-mesenchymal transformation in rats with chronic thromboembolic pulmonary hypertension. Journal of Thrombosis and Thrombolysis. 2021; 52: 454–465.
[23] You W, Wang Z, Li H, Shen H, Xu X, Jia G, *et al*. Inhibition of mammalian target of rapamycin attenuates early brain injury through modulating microglial polarization after experimental subarachnoid hemorrhage in rats. Journal of the Neurological Sciences. 2016; 367: 224–231.
[24] Alexiou K, Wilbring M, Matschke K, Dschietzig T. Relaxin protects rat lungs from ischemia-reperfusion injury via inducible NO synthase: role of ERK-1/2, PI3K, and forkhead transcription factor FKHRL1. PloS One. 2013; 8: e75592.
[25] Walker NM, Belloli EA, Stuckey L, Chan KM, Lin J, Lynch W, *et al*. Mechanistic Target of Rapamycin Complex 1 (mTORC1) and mTORC2 as Key Signaling Intermediates in Mesenchymal Cell Activation. The Journal of Biological Chemistry. 2016; 291: 6262–6271.
[26] Livak KJ, Schmittgen TD. Analysis of relative gene expression data using real-time quantitative PCR and the 2(-Delta Delta C(T)) Method. Methods (San Diego, Calif.). 2001; 25: 402–408.
[27] Chong CZ, Tay ELW, Sia CH, Poh KK. Chronic thromboembolic pulmonary hypertension: a review. Singapore Medical Journal. 2021; 62: 318–325.
[28] Yang J, Madani MM, Mahmud E, Kim NH. Evaluation and Management of Chronic Thromboembolic Pulmonary Hypertension. Chest. 2023; 164: 490–502.
[29] Ranchoux B, Harvey LD, Ayon RJ, Babicheva A, Bonnet S, Chan SY, *et al*. Endothelial dysfunction in pulmonary arterial hypertension: an evolving landscape (2017 Grover Conference Series). Pulmonary Circulation. 2018; 8: 2045893217752912.
[30] Babicheva A, Makino A, Yuan JXJ. mTOR Signaling in Pulmonary Vascular Disease: Pathogenic Role and Therapeutic Target. International Journal of Molecular Sciences. 2021; 22: 2144.
[31] Yang J, Zhou X, Fan X, Xiao M, Yang D, Liang B, *et al*. mTORC1 promotes aging-related venous thrombosis in mice via elevation of platelet volume and activation. Blood. 2016; 128: 615–624.
[32] Meng H, Song W, Liu S, Hsi D, Wan LY, Li H, *et al*. Right Ventricular Diastolic Performance in Patients With Chronic Thromboembolic Pulmonary Hypertension Assessed by Echocardiography. Frontiers in Cardiovascular Medicine. 2021; 8: 755251.
[33] Deng C, Wu D, Yang M, Chen Y, Wang C, Zhong Z, *et al*. Expression of tissue factor and forkhead box transcription factor O-1 in a rat model for chronic thromboembolic pulmonary hypertension. Journal of Thrombosis and Thrombolysis. 2016; 42: 520–528.
[34] Piovella F, D'Armini AM, Barone M, Tapson VF. Chronic thromboembolic pulmonary hypertension. Seminars in Thrombosis and Hemostasis. 2006; 32: 848–855.
[35] Fernandes CJCDS, de Oliveira EP, Salibe-Filho W, Terra-Filho M, Jardim CVP, Kato-Morinaga LT, *et al*. Lung Cavities in Chronic Thromboembolic Pulmonary Hypertension. Clinics (Sao Paulo, Brazil). 2020; 75: e1373.
[36] Tura-Ceide O, Smolders VFED, Aventin N, Morén C, Guitart-Mampel M, Blanco I, *et al*. Derivation and characterisation of endothelial cells from patients with chronic thromboembolic pulmonary hypertension. Scientific Reports. 2021; 11: 18797.
[37] Deng C, Zhong Z, Wu D, Chen Y, Lian N, Ding H, *et al*. Role of FoxO1 and apoptosis in pulmonary vascular remolding in a rat model of chronic thromboembolic pulmonary hypertension. Scientific Reports. 2017; 7: 2270.
[38] Seyfarth HJ, Hammerschmidt S, Halank M, Neuhaus P, Wirtz HR. Everolimus in patients with severe pulmonary hypertension: a safety and efficacy pilot trial. Pulmonary Circulation. 2013; 3: 632–638.
[39] Ogawa A, Firth AL, Ariyasu S, Yamadori I, Matsubara H, Song S, *et al*. Thrombin-mediated activation of Akt signaling contributes to pulmonary vascular remodeling in pulmonary hypertension. Physiological Reports. 2013; 1: e00190.
[40] Di Conza G, Ho PC. ER Stress Responses: An Emerging Modulator for Innate Immunity. Cells. 2020; 9: 695.
[41] Smolders VFED, Lodder K, Rodríguez C, Tura-Ceide O, Barberà JA, Jukema JW, *et al*. The Inflammatory Profile of CTEPH-Derived Endothelial Cells Is a Possible Driver of Disease Progression. Cells. 2021; 10: 737.